



**Modeling glucose isomerization in a packed bed reactor using a new approach to the Briggs-Haldane mechanism**

**Modelado de la isomerización de glucosa en un reactor de lecho empacado utilizando un nuevo enfoque del mecanismo de Briggs-Haldane**

M. Carrasco-Escalante<sup>1</sup>, O. Hernández-Calderón<sup>2</sup>, R. Iribe-Salazar<sup>1</sup>, Y. Vázquez-López<sup>3</sup>, E. Ríos-Iribe<sup>4</sup>, C. Alarid-García<sup>2</sup>, J. Caro-Corrales<sup>1,4\*</sup>

<sup>1</sup>Posgrado en Ciencia y Tecnología de Alimentos, Facultad de Ciencias Químico Biológicas, Universidad Autónoma de Sinaloa, C.P. 80013, Culiacán, Sinaloa, México.

<sup>2</sup>Departamento de Ingeniería Química, Facultad de Ciencias Químico Biológicas, Universidad Autónoma de Sinaloa, C.P. 80013, Culiacán, Sinaloa, México.

<sup>3</sup>Posgrado en Ciencias Agropecuarias, Facultad de Medicina, Veterinaria y Zootecnia, Universidad Autónoma de Sinaloa, C.P. 80260, Culiacán, Sinaloa, México.

<sup>4</sup>Programa Regional de Posgrado en Biotecnología, Facultad de Ciencias Químico Biológicas, Universidad Autónoma de Sinaloa, C.P. 80013, Culiacán, Sinaloa, México.

Received: May 27, 2021; Accepted: August 13, 2021

**Abstract**

Nowadays, immobilized enzymes are utilized in several food industry applications. Some researches use apparent kinetic parameters in immobilized enzyme reactor systems, which are limited to such case studies. To enhance productivity in a packed bed reactor (PBR), a clear description of all the mechanisms (kinetic, intra-particle diffusive mass transport, fluid-particle convective mass transport, and axial dispersion) affecting the process should be established. The objective of this study was to model the isomerization of glucose in a PBR with calcium alginate beads (CAB), using an approach where the kinetic and diffusional mechanisms are described independently. The convective mass transfer ( $k_L$ ) and axial dispersion ( $D_z$ ) coefficients were calculated from correlations. Validation was performed comparing predictions against experimental data ( $R^2 = 0.907$ ) of glucose conversion at the reactor's outlet once steady state was reached. Under the study conditions, in contrast to the effect exerted by diffusive mass transport on fructose specific productivity, the effect of axial dispersion and convective mass transport is negligible. Analyzing different operation parameters via simulation, the particle size had the highest impact on the glucose bioconversion. By reducing the CAB size, the surface area is increased and thus the conversion. It is recommended to test new immobilizing agents or decreasing the CAB size, monitoring that immobilizing support preserves its stability and functionality.

**Keywords:** immobilized glucose-isomerase, packed bed reactor, axial dispersion coefficient, convective mass transfer coefficient.

**Resumen**

Actualmente, las enzimas inmovilizadas se utilizan en numerosas aplicaciones de la industria alimentaria. Algunas investigaciones usan parámetros cinéticos aparentes en sistemas reactores con enzima inmovilizada, los cuales están limitados a esos casos de estudio. Para mejorar la productividad en un reactor de lecho empacado (RLE), se debe establecer una descripción clara de todos los mecanismos (cinético, transporte de masa difusivo intra-partícula, transporte de masa convectivo fluido-partícula y dispersión axial) que afectan el proceso. El objetivo de este estudio fue modelar la isomerización de glucosa en un RLE con perlas de alginato de calcio (PAC), usando un enfoque donde los mecanismos cinético y difusivo son descritos independientemente. Los coeficientes, convectivo de transferencia de masa ( $k_L$ ) y de dispersión axial ( $D_z$ ), se calcularon de correlaciones. La validación se realizó al comparar las predicciones contra datos experimentales ( $R^2 = 0.907$ ) de conversión de glucosa a la salida del reactor, en estado estacionario. En las condiciones de estudio, en contraste con el efecto ejercido por el transporte de masa difusivo sobre la productividad específica de fructosa, el efecto de la dispersión axial y del transporte de masa convectivo es despreciable. Al analizar diversos parámetros de operación, el tamaño de partícula tuvo el mayor impacto sobre la bioconversión de glucosa. Al reducir el tamaño de las PAC aumenta el área superficial y la conversión. Se recomienda probar nuevos agentes inmovilizadores o disminuir el tamaño de las PAC, monitoreando que el agente inmovilizador mantenga su estabilidad y funcionalidad.

**Palabras clave:** glucosa-isomerasa inmovilizada, reactor de lecho empacado, coeficiente de dispersión axial, coeficiente convectivo de transferencia de masa.

\* Corresponding author. E-mail: josecaro@uas.edu.mx  
<https://doi.org/10.24275/rmiq/Cat2474>  
ISSN:1665-2738, issn-e: 2395-8472

## 1 Introduction

---

Glucose isomerase (GI) is widely used to catalyze the isomerization of  $\alpha$ -D-glucose to  $\beta$ -D-fructose, which is part of the production process of high fructose corn syrup, a leading sweetener in food industry (Singh *et al.*, 2020). Over the last decades, this isomerization process has been a subject of study, due to its great commercial importance (Palazzi and Converti, 2001; Dehkordi *et al.*, 2009; Gaily *et al.*, 2013; Selvi and Hariharan 2016; Carrasco-Escalante *et al.*, 2020). The industrial application of the biocatalyst using free GI has numerous disadvantages, such as expensive production cost, low operational stability, meager reusability, among other factors (Neifar *et al.*, 2020).

The immobilization techniques emerged as an alternative, which allows the enzyme to be physically separated from substrate and product for reuse (Junqueira *et al.*, 2019). These procedures involve the protein chain fixation into different supports by using different carrier and coupling techniques, enhancing enzyme stability and reusability (Won *et al.*, 2005; Carrasco-Escalante *et al.*, 2020). Other advantages of immobilized-enzyme systems are: repetitive use of an enzyme in different reactors, improved process control, long half-lives, predictable decay rates, and they are a good model to study *in vivo* kinetics of enzymes (Won *et al.*, 2005). However, there are some subjects about immobilization that should be improved. Among the main drawbacks' highlights are: reduced enzyme load, restricted diffusion of substrate to the enzyme, and low entrapment efficiencies (Homaei *et al.*, 2013). Immobilization of GI has been accomplished and reported using different supports, such as surface-modified alginate beads (Tumturk *et al.*, 2008; Cano-Sampedro *et al.*, 2021), GAMM support (Yu *et al.*, 2011), non-porous glass surface (Chopda *et al.*, 2014), and silica/chitosan hybrid microspheres (Zhao *et al.*, 2016). Among the aforementioned methods, entrapment in calcium alginate beads (CAB) is one of the most typically used supports to immobilize enzymes, due to the high gel strength, low shrinkage, and high permeability of alginates (Tumturk *et al.*, 2008). Moreover, alginate beads are easily available, economic, non-toxic, and biodegradable (Singh *et al.*, 2020).

Immobilized GI is not normally used in a stirred tank reactor (STR), due to its poor resistance to shear stress, where the carrier can be mechanically damaged

and the enzyme dissolved into the substrate solution. In this sense, packed bed reactors (PBR) are of great importance in biochemical industry due to their high yields and efficient product recovery (Aguilar *et al.*, 2005). Among the researches using immobilized GI in a PBR stands out the following: Camacho-Rubio *et al.* (1995) studied the fructose-to-glucose isomerization kinetics using Sweetzyme IT<sup>®</sup> in a recirculation packed bed reactor which enabled them to eliminate the influence of external mass transfer and which could function as a differential reactor when a sufficient flow rate was used; Dehkordi *et al.* (2008) and PonRani and Rajendran (2012) developed different models to describe glucose isomerization kinetics; Rahman *et al.* (2013) made a comparison study of experimental and simulation in the glucose isomerization process, where the model development was based on the diffusion-reaction system, as it involved the heterogeneous system that is in solid-liquid phase; Asif (2015) proposed a retrofitting strategy to enhance the conversion level while significantly reducing the pressure drop in glucose isomerization, and Selvi and Hariharan (2016) developed an analytical algorithm for solving steady state concentration of immobilized GI. Several researches are based on modeling and mathematical simulation to describe the kinetic and diffusion mechanisms, serving as major engineering tools for bioreactors' design and improvement (Che-Galicia *et al.*, 2014).

Nevertheless, some reports used a free enzyme kinetic model to fit experimental data of substrate concentrations in the PBR fluid phase (Dehkordi *et al.*, 2008; Rahman *et al.*, 2013; Gaily *et al.*, 2013); therefore, the convective and diffusional transport effects are incorporated in the kinetic parameters. These kinetic models are called "apparent", whose validity is limited only to those studied conditions. The enzyme immobilization process affects the active-and-available enzyme concentration within the bead (Krishnamoorthi *et al.*, 2015). A large portion of enzyme active sites are deactivated or blocked during the immobilization procedure (Boudrant *et al.*, 2020; Dal Magro *et al.*, 2020). Hence, to obtain a more accurate description of the process, the fraction of residual enzymatic activity (FREA) should be considered. In addition to this, optimization of the isomerization process in a PBR requires the knowledge of diffusive and convective mass transfer resistances. Carrasco-Escalante *et al.* (2020) proposed a new approach to model glucose isomerization, dividing the study in two main steps: (1) the kinetic mechanism was adjusted from a STR using free GI;

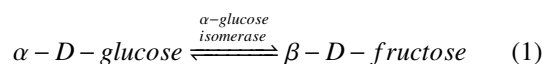
and (2) bioconversion of glucose to fructose was carried out in a STR using immobilized GI in CAB. A mathematical model was developed, taking into account diffusional and kinetic mechanisms within the bead, in which the bioreaction zone is the bead porous network, and it is described in terms of the free enzyme kinetics, the FREA, and the bead effective diffusion coefficient ( $D_{eff}$ ).

The objective of this study was to properly model glucose isomerization in a PBR, using immobilized GI in CAB. The entrapment of enzyme in CAB was used due to the high gel mechanical resistance, low shrinkage and high permeability of alginates. The low conversion of substrate is one of the limitations of using packed-bed reactors, since there is a high resistance to mass transfer within an immobilized biocatalyst bead. Likewise, it is intended to adapt to a PBR the model that Carrasco-Escalante *et al.* (2020) previously validated for a STR; this will be done by including a particle model within a typical packed bed model. Determining a suitable model that describes the glucose isomerization process in a PBR will allow to demonstrate that it is possible to obtain a higher substrate conversion, thus increasing the productivity and reuse of the enzyme compared to a STR. The mathematical modeling of a PBR requires the knowledge of the kinetic mechanism, the diffusive mass transfer mechanism within the particle, as well as, the convective transport mechanism in the fluid-particle interface, and the axial dispersion of the reactants through the reactor fluid phase. The kinetic ( $k_1$ ,  $k_2$ ,  $k_{-1}$ , and  $k_{-2}$ ) and diffusional (FREA and  $D_{eff}$ ) parameters proposed by Carrasco-Escalante *et al.* (2020) were used. The bed porosity was experimentally determined, the convective mass transfer and axial dispersion coefficients were estimated from correlations. The distribution of substrate concentration in the fluid phase was predicted and validated with experimental data, varying enzyme concentration and flow regime. Finally, simulations were carried out to establish the factors that mostly influence productivity in a PBR.

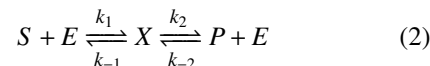
## 2 Mathematical model

### 2.1 Free enzyme

The reversible isomerization of  $\alpha$ -D-glucose to  $\beta$ -D-fructose is defined by the following model



which is successfully described by the Briggs-Haldane mechanism:



The reaction rates for substrate consumption ( $-r_1$ ) and product generation ( $r_2$ ) as function of substrate and product concentrations ( $c_1$  and  $c_2$ ) can be represented as follows (Dehkordi *et al.*, 2009; Gaily *et al.*, 2013; Carrasco-Escalante *et al.*, 2020):

$$-r_1 = r_2 = \frac{\frac{V_{mf}}{K_{mf}}c_1 - \frac{V_{mr}}{K_{mr}}c_2}{1 + \frac{c_1}{K_{mf}} + \frac{c_2}{K_{mr}}} \quad (3)$$

where  $V_{mf}$  and  $K_{mf}$  are the maximum reaction rate and the Michaelis-Menten affinity constant for the glucose to fructose conversion, respectively; while  $V_{mr}$  and  $K_{mr}$  are the analogous parameters for the reverse reaction. The following expressions are used to obtain these parameters:

$$\begin{aligned} V_{mf} &= k_2[E]; & K_{mf} &= \frac{k_{-1} + k_2}{k_1}; & V_{mr} &= k_{-1}[E] \\ K_{mr} &= \frac{k_{-1} + k_2}{k_{-2}}; & K_{eq} &= \frac{V_{mf}K_{mr}}{V_{mr}K_{mf}} \end{aligned} \quad (4)$$

where  $k_1$ ,  $k_2$ ,  $k_{-1}$ , and  $k_{-2}$  are the elementary reaction rates,  $[E]$  is the total enzyme concentration, and  $K_{eq}$  is the reaction equilibrium constant.

### 2.2 Immobilized enzyme

There are some issues that arise through using apparent kinetic parameters: there are limitations related to the diffusive mass transfer; it is not possible to predict the reaction behavior to any modification in the geometry of the immobilizing matrix; different reference volumes (total volume of bioreaction, bead volume, or volume of intraparticle fluid) can be used; the FREA after the immobilization process is unknown. Hence, it is necessary to use a mathematical model that allows to describe separately the effect of the different factors that have a great influence on the reaction and mass transport mechanisms.

The mass transfer within a biocatalytic bead for a chemical species ( $i$ ) can be represented through the following expression (Palazzi and Converti, 2001):

$$\varepsilon_p \frac{\partial c_i}{\partial t} = D_{eff,i} \left( \frac{\partial^2 c_i}{\partial r^2} + \frac{2}{r} \frac{\partial c_i}{\partial r} \right) + \varepsilon_p \hat{r}_i \quad (5)$$

with initial and boundary conditions:

$$t > 0, r = 0, \quad \frac{\partial c_i}{\partial r} = 0 \quad (6a)$$

$$t > 0, r = r_p, \quad -D_{eff,i} \frac{\partial c_i}{\partial r} = k_{L,i}(c_i - C_i) \quad (6b)$$

$$t = 0, 0 \leq r \leq r_p, \quad c_i = c_{i,0} \quad (6c)$$

where  $\varepsilon_p$  is the bead porosity,  $r_p$  is the bead radius,  $\hat{r}_i$  is the volumetric reaction rate based on total volume of bead pores,  $D_{eff,i}$  is the effective diffusion coefficient within the particle,  $C_i$  is the liquid phase concentration, and  $k_{L,i}$  is the fluid-particle convective mass transfer coefficient. The subscript  $i$  indicates the chemical species: glucose ( $i = 1$ ) and fructose ( $i = 2$ ), while the subscript “0” represents an initial condition. Furthermore,  $\hat{r}_i$  is defined from the free enzyme reaction rate ( $r_i$ ), the latter being obtained through kinetic assays using free enzyme.

Contrasting to a free enzymatic reaction system, in which the enzyme is distributed throughout the bioreactor, in an immobilized enzymatic reaction system, all the enzyme is located inside the catalyst bead. Moreover, after the immobilization process, only a fraction of the total enzyme concentration is still active and available to react inside the liquid phase (pores) of the bead (Homaei et al., 2013; Peschke et al., 2019). The effective enzyme concentration,  $[E]_{imm}$  per pore volume within the bead can be estimated based on the total volume of reaction ( $V_t$ ), according to the following expression (Carrasco-Escalante et al., 2020):

$$[E]_{imm} = \frac{\eta m_{E,t}}{\varepsilon_p(1 - \varepsilon)V_t} \quad (7)$$

where  $\eta$  is the FREA,  $m_{E,t}$  is the total mass of immobilized enzyme,  $\varepsilon$  is the volumetric fraction of liquid phase in the reaction system (bed porosity for a PBR), and  $(1 - \varepsilon)V_t$  is equal to the total volume of beads ( $V_p$ ). Therefore, for immobilized and free enzymatic reaction systems, using the same ratio of total enzyme to reaction volume ( $m_{E,t}/V_t$ ), the following relationship is fulfilled:

$$\frac{[E]_{imm}}{[E]} = \frac{\eta}{(1 - \varepsilon)\varepsilon_p} \quad (8)$$

Thus, it is possible to establish, for an immobilized enzymatic reaction system that complies with the ratio,  $[E] = m_{E,t}/V_t$  (ratio between the total mass of catalyst and the total reaction volume), the reaction rate is given as follows (Carrasco-Escalante et al.,

2020):

$$-\hat{r}_1 = \hat{r}_2 = \frac{\frac{\eta}{(1-\varepsilon)\varepsilon_p} V_{mf} \left( c_1 - \frac{c_2}{K_{eq}} \right)}{K_{mf} + c_1 + \frac{K_{mf}}{K_{mr}} c_2} \quad (9)$$

Consequently, it is possible to represent the reaction rate within a bead ( $\hat{r}_i$ ) in terms of the obtained free enzyme reaction rate ( $r_i$ ), which is a better representation for analysis and design purposes, and this can be seen as follows:

$$\hat{r}_i = \frac{\eta}{(1 - \varepsilon)\varepsilon_p} r_i \quad (10)$$

This definition involves the necessity of evaluating the  $\eta$  factor; during the immobilization, a portion of enzyme is affected by the process and the immobilization agent, which deactivates or blocks a number of active sites, diminishing the enzyme activity. Through the FREA calculation, it is possible to approximate the efficiency of the immobilization process. From kinetic assays of free enzyme,  $r_i$  can be determined; and from kinetic assays of immobilized enzyme,  $\eta$  is evaluated. FREA ( $\eta$ ) was previously calculated using a STR under a high hydrodynamic regime (Carrasco-Escalante et al., 2020).

### 2.3 Packed bed reactor modeling

The profile of substrate/product concentration in the fluid phase of a plug flow reactor with axial dispersion can be represented by the following differential equation (Dehkordi et al., 2008; Rahman et al., 2013; Asif, 2015; Selvi and Hariharan, 2016):

$$\varepsilon_b \frac{\partial C_i}{\partial t} = D_z \frac{\partial^2 C_i}{\partial z^2} - U_s \frac{\partial C_i}{\partial z} + (1 - \varepsilon_b) k_L \hat{a}_p (c_{s,i} - C_i) \quad (11)$$

subject to the following initial and boundary conditions:

$$0 \leq z \leq L, t = 0, \quad C_i = C_{i,0} \quad (12a)$$

$$z = 0, t > 0, \quad -D_z \frac{\partial C_i}{\partial z} + C_i U_s = C_{feed,i} U_s \quad (12b)$$

$$z = L, t > 0, \quad \frac{\partial C_i}{\partial z} = 0 \quad (12c)$$

where  $C_i$  is the concentration of the  $i$  species in the fluid phase of the packed bed,  $\varepsilon_b$  is the porosity of the packed bed,  $D_z$  is the axial dispersion coefficient, based on the surface velocity  $U_s$ ,  $k_L$  is the fluid-particle convective mass transfer coefficient,  $\hat{a}_p$  is the specific area of the particle,  $c_{s,i}$  is the concentration of the  $i$  species at the surface of the particle, and  $C_{feed,i}$  is the concentration of the  $i$  species fed to

the reactor. The Danckwerts boundary conditions expressed by Equations (12b-c) takes into account the axial dispersion effect of the reactants at the reactor inlet, and the absence of a substrate concentration gradient at the reactor outlet due to the scarcity of driving force at that point, even when the substrate concentration at the reactor outlet is different from zero (Asif and Abasaed, 1998). Regarding the model of the biocatalytic particle, its expression is given by:

$$\varepsilon_p \frac{\partial c_i}{\partial t} = D_{eff} \left( \frac{\partial^2 c_i}{\partial r^2} + \frac{2}{r} \frac{\partial c_i}{\partial r} \right) + \frac{\eta}{1 - \varepsilon_b} r_i \quad (13)$$

subject to the following initial and boundary conditions:

$$0 \leq r \leq r_p, t = 0, \quad c_i = c_{i,0} \quad (14a)$$

$$r = 0, t > 0, \quad \frac{\partial c_i}{\partial r} = 0 \quad (14b)$$

$$r = r_p, t > 0, \quad -D_{eff} \frac{\partial c_i}{\partial r} = k_L(c_i - C_i) \quad (14c)$$

### 2.3.1 Packed bed physical properties

The mathematical modeling of a packed bed reactor requires the knowledge of bed properties such as porosity, the fluid-particle convective mass transfer coefficient, and the axial dispersion coefficient. Extensive experimental research has been carried out regarding the evaluation of these properties, and they have served to support a set of theoretical relationships that are here presented.

#### 2.3.1.1 Convective mass transfer coefficient

The correlation for a packed bed proposed by Wilson and Geankoplis (1966) is given by:

$$j_m = \frac{1.09}{\varepsilon_b} \text{Re}^{-2/3} \quad (15)$$

where Re is the particle Reynolds number, and  $j_m$  is the Colburn mass transfer coefficient and is defined by the following expression:

$$j_m = \frac{\text{Sh}}{\text{ReSc}^{1/3}} \quad (16)$$

where Sc and Sh are the dimensionless numbers of Schmidt and Sherwood. The three terms of this expression are defined as:

$$\text{Re} = \frac{\rho U_s d_p}{\mu}; \quad \text{Sc} = \frac{\mu/\rho}{D_{AB}}; \quad \text{Sh} = \frac{k_L d_p}{D_{AB}} \quad (17)$$

where  $\rho$  and  $\mu$  are the density and viscosity of the fluid phase, respectively,  $D_{AB}$  is the molecular diffusion

coefficient of the substrate in the fluid phase,  $U_s$  is the surface velocity,  $d_p$  is the particle diameter, and  $k_L$  is the convective mass transfer coefficient.

#### 2.3.1.2 Axial dispersion coefficient

It is necessary to indicate that continuous systems with immobilized enzymes operate at low flow regimes and, hence, mass transfer by dispersion mechanism (in heterogeneous reactors is typically called diffusion) and convection in the fluid phase should be considered with equal importance. The relationship of both transport mechanisms is expressed through the Péclet number. The axial dispersion coefficient in the bioconversion of glucose to fructose was already addressed and reported by Chung and Wen (1968), who under the chosen study conditions in their research, established the following correlation based on Péclet number:

$$\frac{1}{\text{Pe}_z} = \frac{\varepsilon_b}{0.2 + 0.011 \text{Re}^{0.48}} \quad (18)$$

where  $\text{Pe}_z$  is the axial Péclet number and is defined by the following equation:

$$\text{Pe}_z = \frac{U_s d_p}{D_z} \quad (19)$$

Here  $D_z$  is the axial dispersion coefficient of the reactants in the bioreaction fluid phase.

## 3 Materials and methods

### 3.1 Materials

Immobilized GI from a *Streptomyces murinus* strain was used. The enzyme was distributed by Novozymes (Denmark) under Sweetzyme IT<sup>®</sup> trademark. The reported specific dry activity of immobilized GI, according to the manufacturer, was higher than 350 U/g.

### 3.2 Experimental procedures

#### 3.2.1 Experimental apparatus

All experiments were performed in a jacketed packed-bed reaction vertical column ( $d_t = 1.7$  cm,  $L = 75$  cm). The heating system (Thermo Precision, 51221081, USA) was able to adjust the reactor temperature to an accuracy of  $\pm 1$  °C. Hot water was used to maintain constant reactor's temperature. The column was packed with CAB and the substrate

solution flowed down through the reactor by gravity. Volumetric flow rate was controlled using a needle valve. The bottom part of the system was sealed with a cotton layer, to prevent the loss of biocatalyst.

### 3.2.2 Enzyme immobilization

The commercial GI enzyme was initially pulverized to obtain free enzyme particles ( $D = 60$  to  $90 \mu\text{m}$ ). Then, the designated amount of free enzyme (1.25 or 2.5 g) was added into a solution containing sodium alginate (175 mL, 2 % w/v) and 7.0 mL of glutaraldehyde solution (5.0 %), acting as a bifunctional reagent (to improve bead's stability). The solution was slightly stirred and dropped into a 0.3 M  $\text{CaCl}_2$  solution. The resulting spherical CAB ( $d_p = 3 \text{ mm}$ ) were removed and maintained in a diluted solution of 0.3 M  $\text{CaCl}_2$  for 1 day at 4 °C (Verduzco-Navarro *et al.*, 2020). Subsequently, CAB were washed with deionized water and stored at 4 °C (Tumturk *et al.*, 2008; Carrasco-Escalante *et al.*, 2020; Nawaz *et al.*, 2021).

### 3.2.3 Experimental runs

The feed solution (250 mL) was prepared by dissolving the selected amount of glucose in deionized water, then adding 0.7 g of  $\text{MgSO}_4 \cdot 7\text{H}_2\text{O}$  and 0.7 g of  $\text{Na}_2\text{SO}_3$  to stabilize the enzyme and eliminate dissolved oxygen, respectively. The pH was adjusted with 1 N  $\text{H}_2\text{SO}_4$  (Dehkordi *et al.*, 2009; Carrasco-Escalante *et al.*, 2020). In each experimental run, the reactor was packed with CAB and the required inlet conditions were established ( $T = 65 \text{ °C}$ ,  $[S] = 100 \text{ g/L}$ , and  $\text{pH} = 7.5$ ). Samples were taken from the reactor outlet flow every 30 min until the conversion did not change over time (steady state).

### 3.2.4 Analysis method

A refractometer plus polarimeter (ATAGO, RePo-2, Japan) was used to measure glucose and fructose concentrations (Figueroa-García *et al.*, 2021). This device allows to know the percentage of fructose in a sample that may contain glucose, fructose, and sucrose. The determination was based on associating the sample concentration in °Brix with the rotation angle, which is specific for each of these sugars.

## 3.3 Packed bed reactor model

In a PBR, the substrate concentration profile in the fluid phase established in Eq. (11)-(12) represents

Table 1. Kinetic and diffusive parameters for the isomerization of glucose to fructose in a STR using free ( $k_1$ ,  $k_2$ ,  $k_{-1}$ , and  $k_{-2}$ ) and immobilized ( $\eta$  and  $D_{eff}$ ) enzyme.

Parameter	Value
$k_1$	$1.122 \times 10^{-4}$
$k_2$	$3.779 \times 10^{-5}$
$k_{-1}$	$4.705 \times 10^{-5}$
$k_{-2}$	$8.752 \times 10^{-5}$
$K_{eq}$	1.030
$\eta$	0.553
$D_{eff}$	$8.356 \times 10^{-12}$

$k_1$  and  $k_{-2}$  ( $\text{M}^{-1} \text{s}^{-1}$ ),  $k_2$  and  $k_{-1}$  ( $\text{mol g}^{-1} \text{s}^{-1}$ ), and  $D_{eff}$  ( $\text{m}^2 \text{s}^{-1}$ ) (Carrasco-Escalante *et al.*, 2020)

a heterogeneous system composed of a static solid phase (CAB), and a fluid phase (substrate) that travels through the reactor in the  $z$  direction. Simultaneously, within the same system, the reaction rate depends on the reactant concentration profiles into the CAB [Eq. (13)-(14)]. Thus, the system becomes even more complex since there are two arrangements of partial differential equations that rely on  $r$ ,  $z$ , and  $t$ .

Therefore, a proper modeling of enzymatic bioconversion of glucose to fructose using an immobilized enzymatic reaction system, such as PBR, involves the integration of different transport theories with a kinetic mechanism. In this sense, it is necessary to specify: a) the kinetic mechanism, with parameters that are independent of mass transport; b) the intra-particle mass transfer considering the molecular diffusion of the substrate through the pore network; and c) the extra-particle mass transfer, taking into account the axial dispersion of the reactants, and the particle-fluid convective mass transfer.

### 3.3.1 Parameters of the biocatalytic particle model

Concerning to the intra-particle mass transport and kinetic mechanisms, Carrasco-Escalante *et al.* (2020) reported the kinetic and diffusive parameters for glucose-fructose isomerization, using a STR with free and immobilized (CAB) enzyme, respectively. Those parameters are summarized in Table 1 and were used in this study.

### 3.3.2 Determination of packed bed parameters

The description of extra-particle mass transport in a PBR requires the knowledge of the convective mass transfer coefficient ( $k_L$ ) and the axial dispersion

coefficient ( $D_z$ ). In this sense, the correlation proposed by Wilson and Geankoplis (1966) shown in Eq. (15) was used to determine  $k_L$ . On the other hand, to obtain  $D_z$ , the correlation proposed by Chung and Wen (1968) in Eq. (18) was used. In addition, bed porosity ( $\varepsilon_b$ ) was experimentally evaluated for  $d_p = 3$  mm, by measuring the required volume of water to fill up the reactor with a known volume of beads. For other particle sizes, the correlation of Ribeiro et al. (2010) was used.

### 3.3.3 Discretization method

Prior to the numerical solution, the model was written in dimensionless form through the following variable changes:  $\tau = U_S t / d_p$ ,  $\bar{z} = z / d_p$ ,  $\bar{C}_i = C_i / c^0$ ,  $\bar{r} = r / d_p$ , and  $\bar{c}_i = c_i / c^0$ , where  $c^0$  is a reference concentration (glucose concentration at the reactor inlet).

The dimensionless packed bed reactor model was:

$$\varepsilon_b \frac{\partial \bar{C}_i}{\partial \tau} = \frac{1}{\text{Pe}_z} \frac{\partial^2 \bar{C}_i}{\partial \bar{z}^2} - \frac{\partial \bar{C}_i}{\partial \bar{z}} + 6(1 - \varepsilon_b) \text{St}(\bar{c}_{s,i} - \bar{C}_i) \quad (20)$$

subject to the following conditions:

$$0 \leq \bar{z} \leq \frac{L}{d_p}, \tau = 0, \quad \bar{C}_i = \frac{C_{i,0}}{c^0} \quad (21a)$$

$$\bar{z} = 0, \tau > 0, \quad -\frac{1}{\text{Pe}_z} \frac{\partial \bar{C}_i}{\partial \bar{z}} + \bar{C}_i = \bar{C}_{feed,i} \quad (21b)$$

$$\bar{z} = \frac{L}{d_p}, \tau > 0, \quad \frac{\partial \bar{C}_i}{\partial \bar{z}} = 0 \quad (21c)$$

Similarly, the dimensionless particle model is shown in the following equation:

$$\varepsilon_p \frac{\partial \bar{c}_i}{\partial \tau} = \frac{1}{\text{Pe}} \left( \frac{\partial^2 \bar{c}_i}{\partial \bar{r}^2} + \frac{2}{\bar{r}} \frac{\partial \bar{c}_i}{\partial \bar{r}} \right) + (-1)^i \frac{\eta}{1 - \varepsilon_b} \text{Da} \frac{\bar{c}_1 - K_{eq}^{-1} \bar{c}_2}{1 + \frac{c^0}{K_{mf}} \bar{c}_1 + \frac{c^0}{K_{mr}} \bar{c}_2} \quad (22)$$

subject to the following conditions:

$$0 \leq \bar{r} \leq 1, \tau > 0, \quad \bar{c}_i = \frac{C_{i,0}}{c^0} \quad (23a)$$

$$\bar{r} = 0, \tau > 0, \quad \frac{\partial \bar{c}_i}{\partial \bar{r}} = 0 \quad (23b)$$

$$\bar{r} = \frac{1}{2}, \tau > 0, \quad -\frac{\partial \bar{c}_i}{\partial \bar{r}} = \text{Bi}(\bar{c}_i - \bar{C}_i) \quad (23c)$$

where  $\hat{a}_p = 6/d_p$  is the specific surface area for spherical particles,  $\text{Pe}_z = U_S d_p / D_z$  is the Péclet

number of the reactor,  $\text{Pe} = U_S d_p / D_{eff}$  is the Péclet number of the particle,  $\text{St} = k_L / U_S$  is the Stanton number,  $\text{Bi} = k_L d_p / D_{eff}$  is the Biot number, and  $\text{Da} = d_p / (U_S \tau_{mf})$  is the Damköhler number, where  $\tau_{mf} = K_{mf} / V_{mf}$  is the characteristic time scale of the reaction in the fructose production direction. Regarding the discretization procedure, the finite difference method was used (Asif and Abasaed, 1998; Richit et al., 2020). Thus, the domain of the reactor dimensionless mathematical model,  $[0, L/d_p]$ , was discretized into  $N$  segments defined by the coordinates  $[\bar{z}_j, \bar{z}_{j+1}]$  with  $j = 0, 1, \dots, N - 1$ . Consequently, Eq. (20) subject to Eq. (21) was transformed into the following system of ordinary differential equations (ODEs):

$$\frac{d\bar{C}_{i,j}}{d\tau} = \frac{1}{\varepsilon_b \text{Pe}_z} \frac{\bar{C}_{i,j+1} - \bar{C}_{i,j}}{\bar{z}_{j+1} - \bar{z}_j} - \frac{\bar{C}_{i,j} - \bar{C}_{i,j-1}}{\bar{z}_j - \bar{z}_{j-1}} - \frac{1}{\varepsilon_b} \frac{\bar{C}_{i,j+1} - \bar{C}_{i,j-1}}{\bar{z}_{j+1} - \bar{z}_{j-1}} + \frac{6(1 - \varepsilon_b) \text{St}}{\varepsilon_b} (\bar{c}_{s,i,j} - \bar{C}_{i,j}), \quad j = 1, 2, 3, \dots, N - 1 \quad (24)$$

with

$$\tau = 0, \quad \bar{C}_{i,j} = \frac{C_{i,0}}{c^0}, \quad j = 0, 1, 2, \dots, N$$

$$\bar{C}_{i,0} = \frac{\text{Pe}_z(z_1 - z_0) \bar{C}_{feed,i} + \bar{C}_{i,1}}{\text{Pe}_z(z_1 - z_0) + 1}; \quad \bar{C}_{i,N} = \bar{C}_{i,N-1} \quad (25)$$

where  $\bar{z}_{j+1/2} = \frac{1}{2}(\bar{z}_j + \bar{z}_{j+1})$  and  $\bar{z}_{j-1/2} = \frac{1}{2}(\bar{z}_{j-1} + \bar{z}_j)$ . Regarding the domain of the dimensionless mathematical particle model,  $[0, 1/2]$ , was discretized into  $M$  segments defined by the coordinates  $[\bar{r}_k, \bar{r}_{k+1}]$  with  $k = 0, 1, \dots, M - 1$ . As a consequence, Eq. (22) subject to Eq. (23) was transformed into the following system of ODEs:

$$\frac{d\bar{c}_{i,j,k}}{d\tau} = \frac{1}{\varepsilon_p \text{Pe}} \left( \frac{\bar{c}_{i,j,k+1} - \bar{c}_{i,j,k}}{\bar{r}_{k+1} - \bar{r}_k} - \frac{\bar{c}_{i,j,k} - \bar{c}_{i,j,k-1}}{\bar{r}_k - \bar{r}_{k-1}} + \frac{2}{\bar{r}_k} \frac{\bar{c}_{i,j,k+1} - \bar{c}_{i,j,k-1}}{\bar{r}_{k+1} - \bar{r}_{k-1}} \right) + (-1)^i \frac{\eta \text{Da}}{\varepsilon_p (1 - \varepsilon_b)} \frac{\bar{c}_{1,j,k} - K_{eq}^{-1} \bar{c}_{2,j,k}}{1 + \frac{c^0}{K_{mf}} \bar{c}_{1,j,k} + \frac{c^0}{K_{mr}} \bar{c}_{2,j,k}}, \quad k = 1, 2, \dots, M - 1 \quad (26)$$

with

$$\tau = 0, \quad \bar{c}_{i,j,k} = \frac{C_{i,0}}{c^0}, \quad k = 0, 1, 2, \dots, M \quad \bar{c}_{i,j,0} = \bar{c}_{i,j,1}$$

$$\bar{c}_{i,j,M} = \frac{\text{Bi}(\bar{r}_M - \bar{r}_{M-1}) \bar{C}_{i,j} + \bar{c}_{i,j,M-1}}{\text{Bi}(\bar{r}_M - \bar{r}_{M-1}) + 1}; \quad (27)$$

where  $j = 0, 1, 2, 3, \dots, N - 1$ ,  $\bar{r}_{k+1/2} = \frac{1}{2}(\bar{r}_k + \bar{r}_{k+1})$ ,  $\bar{r}_{k-1/2} = \frac{1}{2}(\bar{r}_{k-1} + \bar{r}_k)$ , and  $\bar{c}_{s,i,j} = \bar{c}_{i,j,M}$ . Note there is a particle model for each inner grid point on the reactor domain, which is distinguished by the subscript  $j$ . Concerning to the generation axial and radial coordinates, in the first case, an equidistant mesh was used; while, in the second case, a mesh was used with a variable spacing in the following form:

$$\Delta \bar{r}_1 = \bar{r}_M \frac{1-\varphi}{1-\varphi^M}; \quad \Delta \bar{r}_k = \varphi \Delta \bar{r}_{k-1},$$

$$0 < \varphi < 1, k = 2, 3, \dots, M \quad (28)$$

this due to the concentration variations are higher at the particle surface.

In summary, a system of ODEs with  $(N - 1)M$  equations was generated, which were solved by the Dormand and Prince method (1980). In addition, a mesh independence test was performed, by varying the number of segments of the axial mesh and the radial mesh. It was found that the numerical solution obtained did not vary significantly with the values of  $M = N = 70$ .

### 3.3.4 Simulation of packed bed operating variables

Through steady-state simulations, the effect of the main operating conditions [feed glucose concentration ( $C_{feed,1}$ ) and enzyme concentration  $[E]$  (total mass enzyme/operating reactor volume)] and geometrical properties [biocatalytic bead diameter ( $d_p$ ) and packed bed reactor length ( $L$ )] was evaluated. The base operating parameters used in this study were:  $[E] = 10 \text{ g/L}$ ,  $d_p = 3 \text{ mm}$ ,  $L = 0.75 \text{ m}$ , and  $C_{feed,1} = 100 \text{ g/L}$ . Therefore, for each simulated run, three of these parameters were kept constant, varying one of them as function of the inlet flow rate.

## 3.4 Design of experiments

To validate the proposed PBR model, a two-factor completely randomized design was applied for glucose to fructose conversion in a PBR with immobilized enzyme in CAB. Factors were volumetric flow rate (0.5, 1, 2, and 4 mL/min) and enzyme concentration (5.482 and 10.618 g/L). Fisher's test ( $\alpha = 0.05$ ) was used for means comparison. All tests were performed in triplicate.

Table 2. PBR operation parameters for glucose-fructose isomerization using immobilized enzyme in CAB.

Operation parameter	Value
Number of runs	24
$L$ (m)	0.75
$d_i$ (m)	0.017
$r_p$ (m)	$1.5 \times 10^{-3}$
$T$ ( $^{\circ}\text{C}$ )	65
$\varepsilon_p$ (L/L)	0.919
$\varepsilon_b$ (L/L)	0.343
$\rho_p$ ( $\text{kg/m}^3$ )	1018
$[E]$ (g/L)	5.482, 10.618
$Q$ (mL/min)	0.5, 1, 2, 4
$V$ (L)	0.170
$C_{feed,1}$ (M)	0.556
$C_{feed,2}$ (M)	0

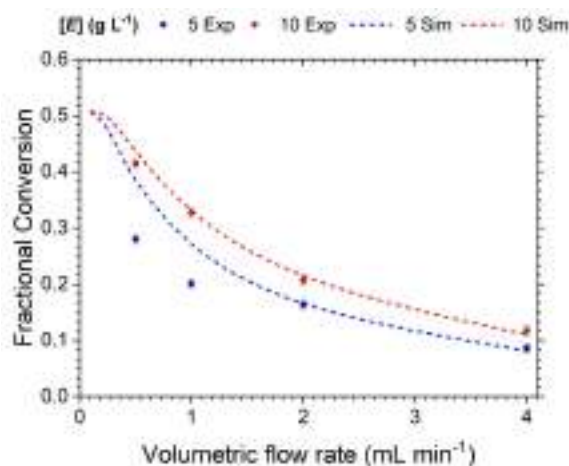


Figure 1. Effect of volumetric flow rate and enzyme concentration in a PBR for the bioconversion of glucose to fructose using immobilized enzyme in CAB (65  $^{\circ}\text{C}$ ,  $[S] = 100 \text{ g/L}$ , and  $\text{pH} = 7.5$ . LSD = 0.0162).

## 4 Results and discussion

### 4.1 Analysis of the bioconversion in a PBR

The kinetic and diffusion parameters reported by Carrasco-Escalante *et al.* (2020) using a STR with free and immobilized enzyme (Table 1) were used to simulate the bioconversion as function of volumetric flow rate at different enzyme concentrations in a PBR (Figure 1). The operating parameters used to calculate  $k_L$  and  $D_z$  by correlations [Eq. (15) and Eq. (18)] are shown in Table 2, some of which

were evaluated experimentally. The initial glucose and fructose concentrations within the catalyst bead were considered negligible. The bulk density ( $\rho_p$ ) and porosity ( $\varepsilon_p$ ) of the gel beads ( $d_p = 3$  mm) were reported by Carrasco-Escalante *et al.* (2020).

Figure 1 shows the experimental results of the effect of volumetric flow rate and enzyme concentration on the bioconversion of glucose to fructose using a PBR. Experimental data were taken once steady state was reached. With an increase in volumetric flow rate, the conversion fraction decreases (Santana *et al.*, 2020). This is a predictable behavior and may be explained by a decrease in mean residence time of the glucose solution into the PBR. The mathematical model, discretized by finite differences [Eqs. (24)-(28)] and integrated by the Dormand and Prince method, was validated with experimental data (Figure 1). Enzyme concentration was set as  $m_{E,t}/V_t$  (5 and 10 g/L). An adequate relation between simulated and experimental data was obtained ( $R^2 = 0.907$ ). However, at low flow regimes (0.5 and 1 mL/min) and the lowest level of enzyme concentration (5.482 g/L), the comparison between the simulated and experimental data showed differences. This may be due to the struggle that implies establishing such small volumetric flow rates at experimental level. As the latter increases, it becomes easier to stabilize, thereby greatly reducing the experimental error.

Table 3 shows a comparison of glucose-fructose conversion in three different reaction systems. In STR systems with free and immobilized enzyme, the experiment was limited to 210 minutes. In contrast, in the PBR, the evaluation was carried out until the steady state was achieved. The required time in a PBR varied according to the selected inlet flow (around 2 hours for 4 mL/min up to 10 hours for 0.5 mL/min). Table 3 shows that the conversion achieved in the PBR (0.414) is higher when compared to STR (0.312) with immobilized enzyme in CAB; however, the required time was almost triplicated (Santana *et al.*, 2020). Nevertheless, the main advantage of a PBR lies in bead

stability, due to the use of smaller flow rates, which promotes the reuse capability, since bead mechanical damage is almost negligible (Zhang *et al.*, 2020).

The convective mass transfer and axial dispersion coefficients ranged from:  $k_L = 4.1 \times 10^{-6}$  to  $8.2 \times 10^{-6}$  m/s and  $D_z = 1.8 \times 10^{-7}$  to  $1.4 \times 10^{-6}$  m<sup>2</sup>/s, respectively. These parameters were adequate to predict the bioreactor behavior and are in concordance with reports in literature. Using data reported by Dehkordi *et al.* (2008), the  $k_L$  and  $D_z$  parameters were calculated and ranged from  $k_L = 4.0 \times 10^{-5}$  to  $1.0 \times 10^{-4}$  m/s and  $D_z = 4.8 \times 10^{-6}$  to  $5.0 \times 10^{-5}$  m<sup>2</sup>/s in a PBR for glucose to fructose isomerization. The difference in the coefficients can be attributed to the inlet flows used in the present study (0.5-4 mL/min) in comparison to Dehkordi *et al.* (2008) (40-275 mL/min), due to  $k_L$  and  $D_z$  are strongly affected by the flow regime, and tend to rise as the flow rate is increased.

## 4.2 Effect of packed bed operating variables

### 4.2.1 Operating conditions

Figure 2a shows the simulated conversion fraction of glucose, as a result of different  $[E]$ . As expected, increasing  $[E]$  promoted an improvement on fructose production. Nevertheless, this outcome is less accentuated at high flow regimes. Moreover, the effect of  $[E]$  is almost negligible for  $Q > 8$  mL/min. Analyzing the fructose specific productivity (molar flow of generated fructose per mass of used enzyme) for all the simulations (Figure 2b), the highest variation in productivity occurs from 0.1-2 mL/min, and the best efficiency of used enzyme occurs at the lowest enzyme concentration in the reactor:  $[E] = 2.5$  g/L. Thus, although a higher enzyme concentration improves glucose conversion at the reactor outlet (higher outlet fructose concentration), this leads to a decrease in specific productivity and, therefore, to a waste of the used enzyme.

Table 3. Maximum conversion fraction achieved for glucose-fructose isomerization at different reaction systems (65 °C and  $[S] = 100$  g/L).

Reaction system	Reaction residence time (min)	$[E]$ (g/L)	Conversion fraction	Authors
STR Free enzyme	210	10	$0.508 \pm 0.0015$	Carrasco-Escalante <i>et al.</i> (2020)
STR Immobilized enzyme (CAB)	210	6.292	$0.312 \pm 0.0038$	Carrasco-Escalante <i>et al.</i> (2020)
PBR Immobilized enzyme (CAB)	600	10.618	$0.414 \pm 0.0028$	

Note: The same enzyme mass was used in all cases (2.5 g).

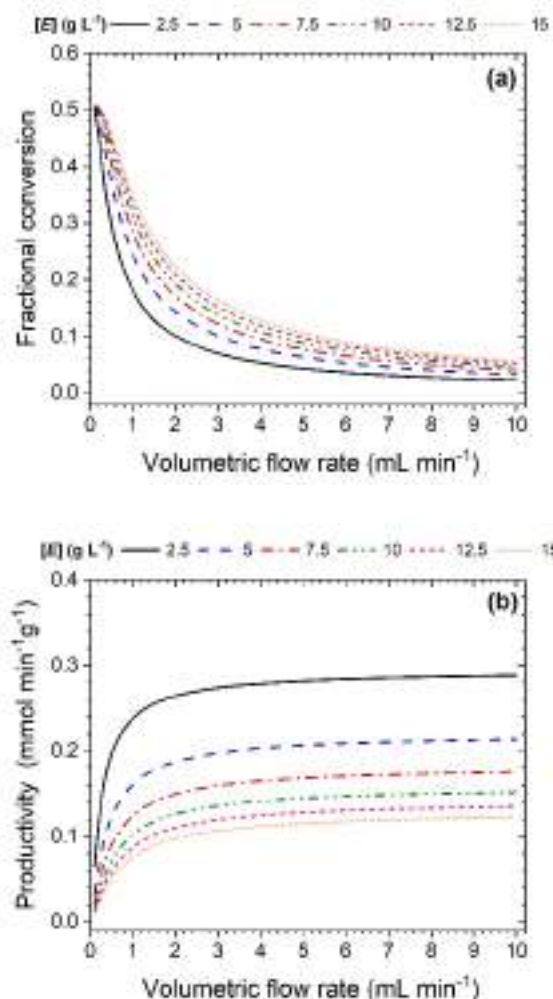


Figure 2. Effect of enzyme concentration on (a) glucose to fructose conversion and (b) specific productivity of fructose, using a PBR at 65 °C,  $[S] = 100$  g/L, and  $\text{pH} = 7.5$ .

The effect of feed glucose concentration is shown in Figure 3a. It may be noticed that  $C_{feed,1}$  was the factor that exerted the least impact on the bioconversion process. Basically, it was found that lower  $C_{feed,1}$  turns to better conversions. The latter is possibly due to the nature of the isomerization kinetics, since, at a higher  $C_{feed,1}$ , the reaction rate is reduced, leading to lower glucose conversions. On the other hand,  $C_{feed,1}$  exerts a greater effect on productivity (Figure 3b), which increases as  $C_{feed,1}$  is raised. This is due to a higher concentration gradient between the fluid phase and the biocatalytic bead surface, promoting higher flows

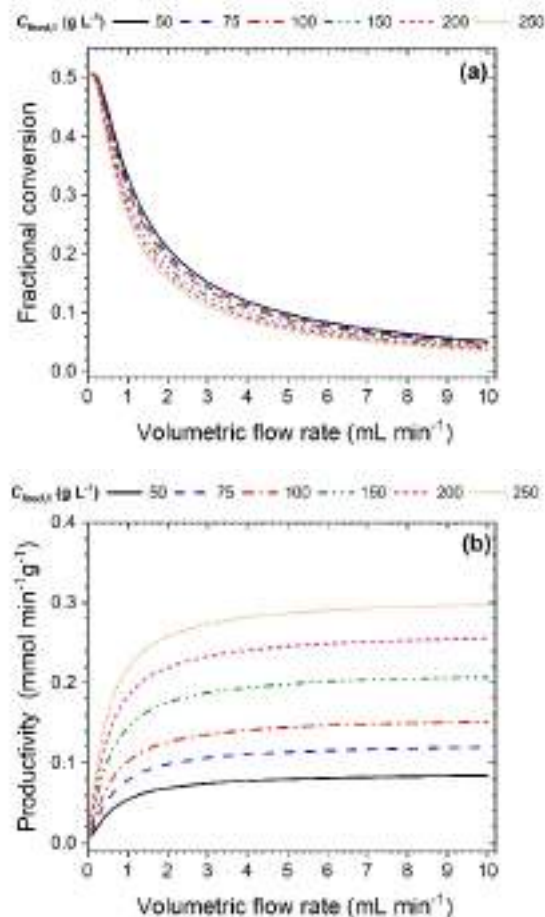


Figure 3. Effect of feed glucose concentration on the (a) glucose to fructose conversion and (b) specific productivity of fructose, using a PBR at 65 °C,  $[E] = 10$  g/L, and  $\text{pH} = 7.5$ .

of reactants within the biocatalytic bead, and thus, higher flows of the generated product. The latter leads to higher productivities, as the enzyme mass and the bed volume remained constant during the simulations.

#### 4.2.2 Geometrical properties

The impact of catalytic bead diameter ( $d_p$ ) is shown in Figure 4. As the flow rate increases, the conversion decreases, as well as, the smaller particle size, the higher the conversion (Figure 4a). This latter behavior can be attributed to an increased surface area/volume ratio (Peschke *et al.*, 2019). Therefore, considering that bioreaction occurs mainly on the bead surface due to the high intraparticle diffusional resistance, the effect of bead size is very important on the bioconversion process. In fact, the highest gradient in

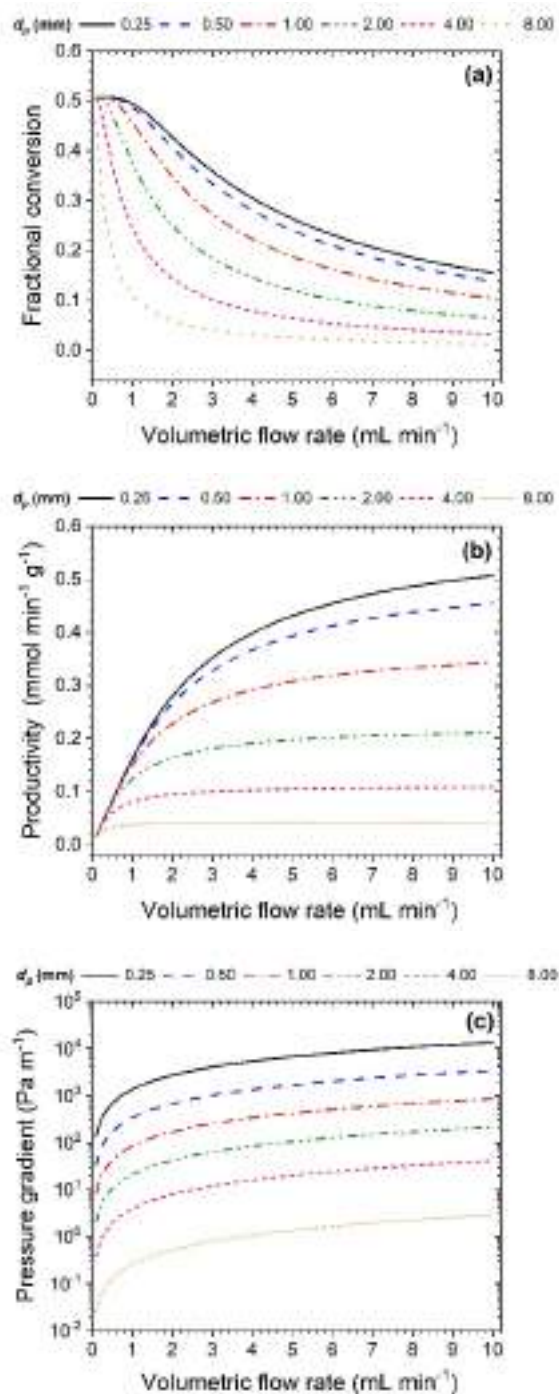


Figure 4. Effect of particle diameter on (a) glucose to fructose conversion, (b) specific productivity of fructose, and (c) pressure gradient, using a PBR at 65 °C,  $[S] = 100$  g/L,  $[E] = 10$  g/L, and  $\text{pH} = 7.5$ .

glucose conversion, when different bead sizes were used, was achieved at volumetric flow rates from

0.1-2 mL/min for large particle diameters; while for the smallest particle diameter, the conversion was very close to the maximum allowable conversion in the aforementioned range of volumetric flow. On the other hand, when determining the fructose specific productivity, it was found that the smaller the particle diameter, the higher the productivity achieved (Figure 4b). Hence, the use of large particles represents a waste of catalyst, because the center of those particles does not contribute to the overall glucose isomerization process. In all the numerical experiments, there is a more pronounced increase in the specific productivity at low volumetric flows (0.1-2 mL/min), which is the result of the effect of flow regime on the advective transport of the chemical species throughout the bioreactor.

Certainly, under this analysis, the selection of the smallest bead diameter demonstrates to be the most suitable choice, with the aim of improving glucose conversion. In addition, this geometrical parameter does not require a higher amount of enzyme during the bioreaction process, but it brings a considerable improvement on the conversion and fructose productivity. However, a smaller bead size requires higher pressure gradients to induce the flow through the bed, which promotes high shear stresses into the beads. Furthermore, beads could be mechanically damaged, causing a reduction in size to a level where they could be dragged at the reactor outflow. Figure 4c shows the effect of particle diameter on pressure gradient ( $\Delta p/L$ ) along the packed bed reactor. This pressure gradient was calculated using the Ergun correlation (Bird *et al.*, 2006) and the correlation of Ribeiro *et al.* (2010). Particles of small diameter (0.25 mm) are subjected to pressure gradients in the order of  $10^3 - 10^4$  Pa/m for volumetric flow rates higher than 2 mL/min, while particles of conventional diameter (2 mm) are affected by pressure gradients in the order of 10-100 Pa/m. Thus, although the 0.25 mm diameter bead offers the best specific productivity, operationally, this particle size selection can be prohibitive due to the rapid mechanical damage that beads will suffer from the pressure gradients required to drive workflow. Therefore, the bead mechanical resistance should be a subject of study, to select the smallest possible diameter in which CAB retain their functionality.

Figure 5a shows the impact of the packed bed length, which exerts a positive effect on the glucose conversion; this due to an increase in residence time. However, the increase in reactor length leads to the use of higher quantities of enzyme; because the enzyme

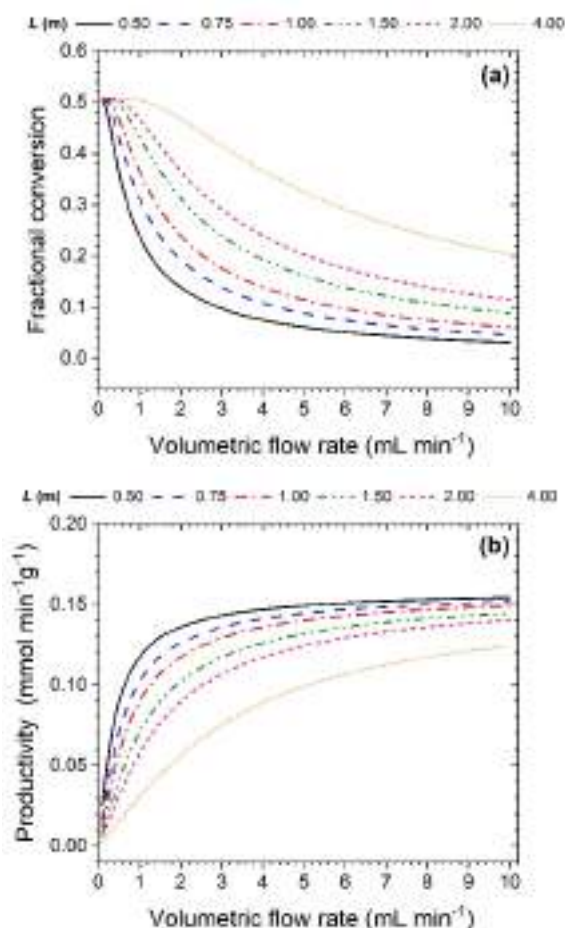


Figure 5. Effect of packed bed length on (a) glucose to fructose conversion and (b) specific productivity of fructose at 65 °C,  $[S] = 100 \text{ g/L}$ ,  $[E] = 10 \text{ g/L}$ , and  $\text{pH} = 7.5$ .

mass/bed volume ratio remained constant. Hence, this increase can be a good alternative, when it is intended to achieve higher glucose conversions at high volumetric flow rates. At short packed bed lengths, the highest glucose conversion variation was achieved in the range of 0.1 to 2 mL/min. While at long packed bed lengths, the conversion achieved is very close to the maximum allowed conversion with flow rates ranging from 0.1-2 mL/min; above that range, a conversion decrease occurs with the variation of the volumetric flow rate. Specific productivity increases (Figure 5b) as packed bed lengths are shorter, as well as flow rates are higher. On the other hand, regardless of the packed bed length, by increasing the volumetric flow rate, the productivities become asymptotical and are very similar to each other. For short bed lengths, the highest variation in productivity

also occurs from 0.1-2 mL/min. As the packed bed length increases, the variation in productivity becomes slower with the variation in volumetric flow rate. The tendency to reach similar productivities as the flow rate increases, for the different packed bed lengths, is due to the longer the packed bed length, the higher the volumetric flow required to achieve the concentrations of reactants throughout the reactor be similar to feed concentrations.

#### 4.2.3 Mass transfer coefficients

Two simulation sets were carried out using particle diameters of 0.5, 1, and 2 mm and volumetric flow rates from 0.1-10 mL/min: (a) first, neglecting the effect of axial dispersion ( $D_z = 0$ ); and (b) second, neglecting the convective mass transfer resistance ( $k_L \rightarrow \infty$ ). These two sets of simulations were compared with the set of simulations in which both the effect of axial dispersion and convective mass transfer are considered. In this comparison, the percentage deviation of the specific fructose productivity was calculated and is shown in Table 4. The axial dispersion and external mass transfer resistance do not exert a high impact on specific productivity, under the used operating and geometric conditions. All percentage deviations are less than 1 %, with a tendency to increase as the particle diameter and volumetric flow rate increase. In this sense, it is possible to dispense with both mass transport phenomena in the mathematical modeling of the fixed-bed reactor, under the studied conditions.

Finally, the effect that the intra-particle mass transfer resistance exerts on the fructose specific productivity at different particle sizes (1, 2, and 4 mm) and volumetric flow rates (0.1-10 mL/min) was analyzed. Two simulation sets were carried out varying the experimentally obtained effective diffusion coefficient:  $2D_{eff}$  and  $10D_{eff}$  (Figure 6). For 1 mm particles, productivity had a higher change when the effective diffusion coefficient was doubled than when it was tenfold; while for 4 mm particles, the change in productivity was more important when the effective diffusion coefficient was tenfold than when it was doubled. Due to the high intraparticle resistance, the penetration length of the chemical species into the bead is short; therefore, productivity is favored in systems when particle size is decreased due to the increase in the specific area ( $\hat{a}_p$ ). However, bed porosity also decreased, causing the catalyst concentration within the bead to diminish too, due to the raise in the used bead volume. This is because, if

Table 4. Percentage deviation of fructose specific productivity neglecting (1) axial dispersion and (2) external resistance to mass transfer within the bead, in comparison to simulations in which both mass transport phenomena are considered.

Flow rate (mL/min)	$D_z = 0$			$k_L \rightarrow \infty$		
	0.5 mm	1.0 mm	2.0 mm	0.5 mm	1.0 mm	2.0 mm
0.1	0.016	0	0.006	0	0.003	0.042
0.2	0.016	0	0.016	0	0.002	0.009
0.3	0.014	0.003	0.086	0	0.003	0.044
0.4	0.001	0.015	0.186	0.001	0.01	0.07
0.5	0.001	0.035	0.283	0.003	0.02	0.082
0.6	0.007	0.06	0.364	0.007	0.029	0.085
0.7	0.014	0.087	0.429	0.01	0.036	0.081
0.8	0.021	0.113	0.48	0.013	0.04	0.075
0.9	0.029	0.137	0.52	0.016	0.042	0.07
1	0.036	0.158	0.551	0.018	0.043	0.065
2	0.087	0.264	0.65	0.027	0.049	0.077
3	0.105	0.287	0.641	0.051	0.086	0.128
4	0.111	0.29	0.618	0.089	0.132	0.175
5	0.113	0.286	0.558	0.131	0.176	0.216
6	0.112	0.28	0.578	0.171	0.215	0.271
7	0.111	0.274	0.483	0.207	0.249	0.25
8	0.109	0.267	0.596	0.239	0.278	0.292
9	0.107	0.261	0.521	0.268	0.303	0.314
10	0.105	0.255	0.51	0.293	0.324	0.332

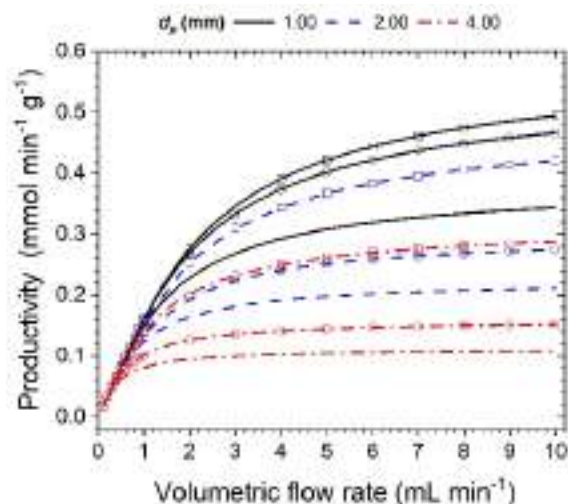


Figure 6. Effect of intraparticle effective diffusion coefficient on the specific productivity of fructose with different particle diameters (1, 2, and 4 mm), using a PBR at 65 °C,  $[S] = 100$  g/L,  $[E] = 10$  g/L, and pH = 7.5. (o)  $2 D_{eff}$ , ( $\square$ )  $10 D_{eff}$ .

the design parameter  $[E]$  (mass of catalyst per volume of reactor) is wanted to keep constant, as well as

the reactor volume, then, the same mass of catalyst should be used. Nonetheless, the increase in bead volume caused by reducing particle size causes the enzyme concentration inside the bead to diminish. Enzyme concentrations in the beads (mass of catalyst per bead volume), for diameters  $d_p = 1, 2,$  and  $4$  mm, were  $[E]_{imm} = 15.95, 15.97,$  and  $16.68$  g/L, respectively, when enzyme concentration was  $[E] = 10$  g/L. In this sense, the reduction of particle size has a positive effect (increase in  $\hat{a}_p$ ) and a negative effect (decrease in  $[E]_{imm}$ ) on the specific productivity, which in a net way, the raise in specific area is more important. Regarding the effect that the flow regime exerts on conversion and productivity, high volumetric flow rates favor a higher glucose concentration throughout the reactor, and with this, the glucose concentration in the particle surface increments, and the molar flow of fructose leaving the reactor also increases. However, the reactor outlet stream has a low fructose concentration (low glucose conversion), which is an unacceptable operating condition. On the other hand, at low volumetric flow rates, the residence time of the reaction system is raised, which improves bioreaction conversion, and therefore, a higher fructose concentration at the bioreactor outlet is

obtained. Given the external resistance is not a limiting transport mechanism, the design recommendation is to operate the bioreactor at low volumetric flow rates and using small particle sizes, taking care to avoid excessive pressure gradients, as well as to improve the immobilization technique to raise the effective diffusion within the particle.

### 4.3 Simulation of the transient state

The effect exerted by the Reynolds, Damköhler, and particle Péclet numbers, as well as initial substrate/product concentration within the particle, on the required time to achieve the bioprocess steady state was analyzed. This analysis arises as it was found flow regime, reaction rate, and diffusion of reactants inside the particle, exert the highest effect on the conversion. It was considered the bioprocess reached the steady state when conversion at the bioreactor outlet accomplished 99 % of the maximum achieved conversion under each simulated condition. The maximum conversion was determined by comparing the conversions of two simulations with long process times, whose relative variation was less than 0.1 %. In addition, for comparison purposes, the reference simulation was performed under the following conditions:  $T = 65\text{ }^{\circ}\text{C}$ ,  $C_{feed,1} = 0.556\text{ M}$ ,  $[E] = 10\text{ g/L}$ ,  $\text{Re} = 0.1$ ,  $\text{Da} = 0.01$ , and  $\text{Pe} = 10,000$ .

Figure 7a shows the effect the flow regime exerts on the conversion during the transient state of the bioprocess. The higher the flow regime, the longer the dimensionless time required to reach the steady state. This is due to the Damköhler and particle Péclet numbers remain constant while the variation of the Reynolds number is carried out; thus, the bead diameter and the surface velocity of the fluid phase are different in each simulation, ranging from  $0.447\text{ mm} < d_p < 4.472\text{ mm}$  and  $2.236 \times 10^{-5}\text{ m/s} < U_S < 2.236 \times 10^{-4}\text{ m/s}$  ( $0.30\text{ mL/min} < Q < 3.05\text{ mL/min}$ ). It was found that the higher the Reynolds number, the larger the particle diameter and the higher the surface velocity of the reactor fluid phase. Thus, at a higher flow regime, the substrate concentration in the fluid phase tends to be equal to the feed substrate concentration, promoting a high substrate concentration on the external surface of the biocatalytic beads, which leads to a high intraparticle substrate concentration profile. In addition, due to, in the reference simulation, the initial concentration of reactants is zero, the required time to reach steady state is controlled by the time needed for accumulation of reactants inside the biocatalytic beads. Furthermore, under these circumstances, the biocatalytic beads are

larger, which increase the penetration length of the reactants into the bead, what implies a longer time for the diffusional mobility of the reactants. Other effects that result from the variation of particle size are added; such as the variation of bed porosity and enzyme concentration within beads, due to the bed volume and the used enzyme mass were kept constant. Some important particular times, in this comparison of results, are the residence time within the reactor ( $\tau_{bed} = L/U_S$ ), the characteristic time scale of the reaction ( $\tau_{mf} = K_{mf}/V_{mf}$ ), and the required time to reach the steady state ( $\tau_{st}$ ), they were:  $0.93\text{ h} < \tau_{bed} < 9.32\text{ h}$ ,  $\tau_{mf} = 0.56\text{ h}$ , and  $3.50\text{ h} < \tau_{st} < 5.03\text{ h}$ , respectively. Note there is another characteristic time: the time required for a fluid element to move in the fluid phase from one particle extreme to the other in the axial direction,  $\tau_{part} = d_p/U_S$ ; in a more simplistic way, it can be referred to as a characteristic contact time between the fluid phase and the bead. Thus, this characteristic time was the same for all simulations:  $\tau_{part} = 20\text{ s}$ , because the Damköhler number remained constant in this set of simulations,  $\text{Da} = 0.01$ . Finally, it can also be defined a characteristic time related to the intraparticle diffusional mobility of the reactants,  $\tau_{diff} = d_p^2/D_{eff}$ , which was  $\tau_{diff} = 55.56\text{ h}$ , due to the particle Péclet number also remained constant.

The effect that the variation of the Damköhler number ( $\text{Da} = \tau_{part}/\tau_{mf}$ ) exerts on the conversion during the transient state of the bioprocess is shown in Figure 7b. The lower the Damköhler number, the longer the dimensionless time required to reach the steady state. Although technically, the characteristic reaction time can be modified by varying the reaction temperature; in this study, it was decided to keep it constant ( $\tau_{mf} = 0.56\text{ h}$ ). Instead, the contact time between the fluid phase and the bead was varied ( $\tau_{part}$ ) through the change in particle size and surface velocity of the fluid phase, but keeping the Reynolds and particle Péclet numbers constant ( $\text{Re} = 0.1$  and  $\text{Pe} = 10,000$ ). This caused a variation in the bead diameter from 1-4 mm and in the superficial velocity from  $2.5 \times 10^{-5}$ - $1.0 \times 10^{-4}\text{ m/s}$  ( $0.34$ - $1.36\text{ mL/min}$ ). Thus, the higher the Damköhler number, the less dimensionless time required to reach the steady state, despite the particle diameter increases and the surface velocity decreases. The reason for this is that the higher the Damköhler number, the larger the characteristic time scale ( $\tau_{part} = d_p/U_S$ ) used to dimensionless the system, which ranged from 10-160 s. The dimensional times required to achieve steady state ranged from 3.56-16.55 h, having the shortest

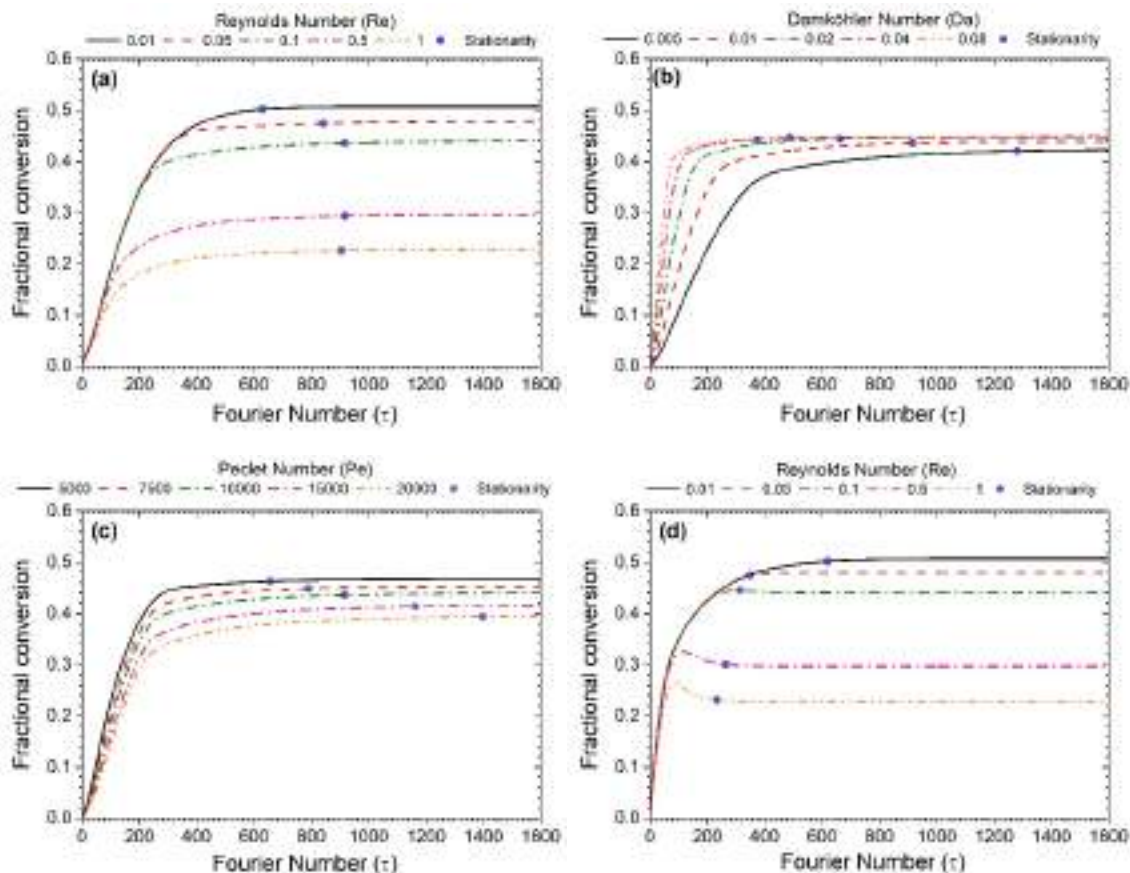


Figure 7. Fractional conversion behavior during the transient state for (a) Reynolds number with  $c_{1,0} = c_{2,0} = 0$ , (b) Damköhler number, (c) particle Péclet number, and (d) Reynolds number with  $c_{1,0} + c_{2,0} = 0.556 \text{ M}$  and  $c_{2,0}/c_{1,0} = K_{eq}$ .

time when the Damköhler number was the smallest, which corresponds to the simulation with the smallest bead size and the highest surface velocity. On the other hand, the characteristic diffusion time ( $\tau_{diff}$ ) ranged from 28–444 h, while the reactor residence time ( $\tau_{bed}$ ) from 2.08–8.33 h.

Regarding the effect that the variation of the particle Péclet number exerts on the conversion during the transient state of the bioprocess (Figure 7c), it was found that the higher the Péclet number, the higher the dimensionless time required to reach the steady state. This is because raising the Péclet number, the resistance to intraparticle mass transfer increases. In this case, the characteristic contact time scale remained constant for all simulations:  $\tau_{part} = 20 \text{ s}$ , and in this sense, the dimensional time required to reach the steady state is also longer when the Péclet number is higher. Thus, the Péclet variation was the direct result of the change in the effective diffusive

coefficient ( $5 \times 10^{-12} - 2 \times 10^{-11} \text{ m}^2/\text{s}$ ). The particle diameter and the surface velocity remained constant:  $d_p = 1.41 \text{ mm}$  and  $U_s = 7.07 \times 10^{-5} \text{ m/s}$ , ( $Q = 0.96 \text{ mL/min}$ ), for this set of simulations. Additionally, the characteristic diffusion time ( $\tau_{diff}$ ) ranged from 28–111 h and to achieve steady state from 3.64–7.76 h, while the residence time of the reactor ( $\tau_{bed}$ ) was 2.95 h.

Another factor that affects the time required to achieve steady state is the initial concentration of reactants within the particle. All the previous simulations correspond to a situation where the beads have been used for the first time; therefore, the concentration of reactants inside the bead is zero. However, when the beads are reused, the reactant concentration is not zero, and they have a concentration close to equilibrium with respect to the feed concentration, as long as the reused beads have only been rinsed between one and another

experimental run, and a considerable period of time has elapsed between both runs to achieve chemical equilibrium. Thus, the simulations in which the flow regime was varied were repeated, but now considering that the initial intraparticle concentration corresponds to the equilibrium conditions with respect to a glucose solution of 100 g/L. When comparing the simulations with the same flow regime of Figures 7a and 7d, a decrease in the time required to achieve steady state was observed when the beads are reused with their intraparticle reactants in equilibrium. This is because the time required to readjust the concentration profiles of the reactants inside the reused bead is shorter than that when the beads are used for the first time; because in the latter case, a higher diffusional mobility of reactants between the fluid phase and the biocatalytic beads is required. In addition, the time required to achieve steady state decreases as the Reynolds number increases; as at high flow rates of the reactor fluid phase, low fructose and high glucose concentrations predominate throughout the reactor, promoting a higher driving force in the mass transfer of the reactants between the fluid phase and the catalytic beads. Regarding the times required to achieve steady state, these ranged from 1.30-3.44 h.

#### 4.4 Effect of $Re$ , $Da$ , and $Pe$ numbers on conversion

Reviewing the effect that the Reynolds number exerts on conversion (Figure 8a-c), it was generally found that, the higher the Reynolds number, the lower the conversion. By increasing the flow regime, the concentrations of the reactants in the fluid phase throughout the reactor become similar to the conditions of feed concentration, which favors a high concentration of substrate on the bead surface, and with it, a higher fructose production rate within the bead. However, the high flow of the fluid phase decreases the residence time of the fluid phase, causing a low glucose concentration at the reactor outlet and, therefore, a low conversion. Regarding the Damköhler number, it is observed that the conversion varies more rapidly with respect to the Reynolds number from 0.01-0.1, as the Damköhler number diminishes. However, conversion decreases more rapidly with respect to the Reynolds number from 0.1-1, as the Damköhler number is raised. This is because at higher Damköhler numbers, the increase in the Reynolds number exerts a more important effect on particle size and, in consequence, on bed porosity. For example, using  $Pe = 5000$  at  $Da = 0.005$ , the Reynolds number

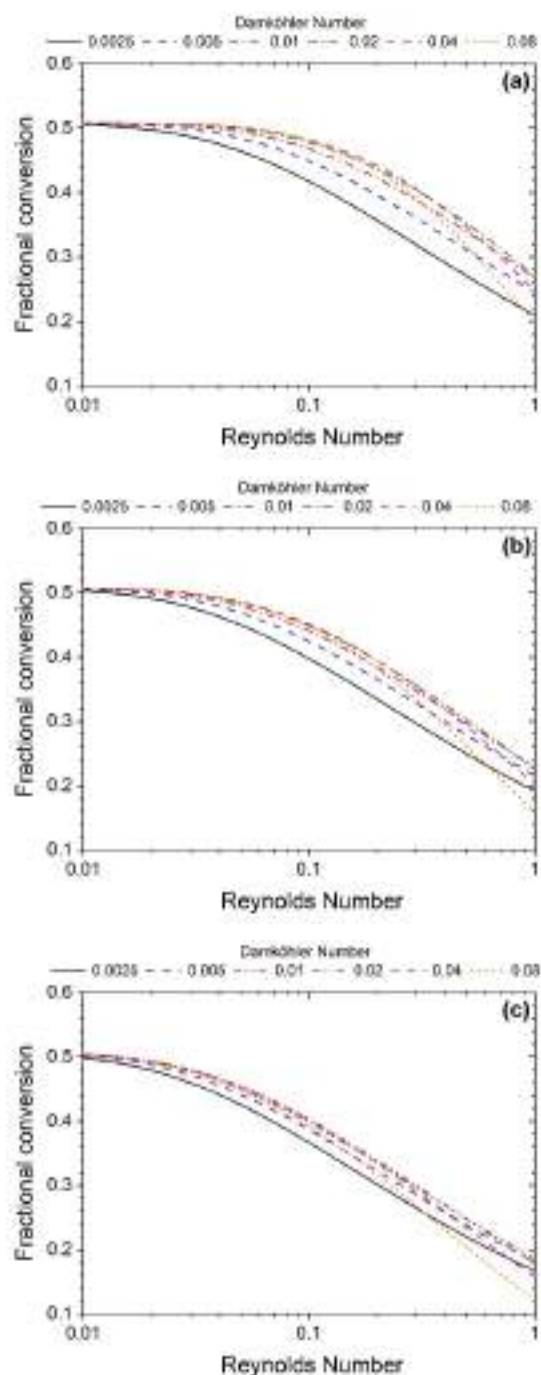


Figure 8. Behavior of the fractional conversion in steady state as a function of the Reynolds, Damköhler, and particle Péclet number. (a)  $Pe = 5000$ , (b)  $Pe = 10,000$ , and (c)  $Pe = 20,000$ .

variations from 0.01-0.1 and 0.1-1 led to a bed porosity variation from 0.373-0.373 and 0.373-0.384, respectively; while at  $Da = 0.08$ , the variations of the

Reynolds number from 0.01-0.1 and 0.1-1 led to a variation of bed porosity from 0.373-0.401 and 0.401-0.676, respectively. In this sense, although the raise in bed porosity leads to an increase in the intraparticle enzyme concentration (due to bed volume and enzyme mass remained constant), the reduction in the particle specific area becomes the more important effect on conversion. On the other hand, the increment in Péclet number causes the effect the Damköhler number exerts on the conversion to decrease; and in general, promotes a conversion reduction, due to the raise in the internal resistance; in this sense, the particle size is no longer a predominant factor to improve the productivity, as occurs at low Péclet numbers.

#### 4.5 Effect of particle size on transport mechanisms

In addition, the effect that particle diameter exerts on the different mass transport mechanisms (diffusive and convective mass transport, and axial dispersion) via dimensionless numbers was analyzed. The Péclet number was little influenced by both particle size and flow regime variations (Figure 9a), which indicates that the effects of axial dispersion were of the same magnitude, in all the numerical experiments carried out. On the other hand, the Stanton number (Figure 9b) and the mass Biot number (Figure 9c) are strongly dependent on both particle size and flow regime. Regarding the behavior of the Stanton number, it is evident that particle size considerably affects the convective mass transfer coefficient ( $k_L$ ), and that the flow regime exerts a greater influence on the advective transport (bulk transport) of the chemical species, throughout the reactor, than on the external convective mass transport. In more detail, the most pronounced variation of the Stanton number occurred at low flow regimes (0.1-2 mL/min), a similar effect was found on the behavior of specific productivity. In all cases, large mass Biot numbers were obtained, indicating the particle internal resistance mainly controls mass transfer. In general, the larger the particle diameter, the higher the Biot number; therefore, the higher the diffusion resistance within the particle. Regarding the effect of the flow regime on the Biot number, as the volumetric flow rate raises, the Biot number increases; this as a result of the positive effect that the bulk fluid velocity ( $U_S$ ) exerts on the convective mass transfer coefficient ( $k_L$ ).

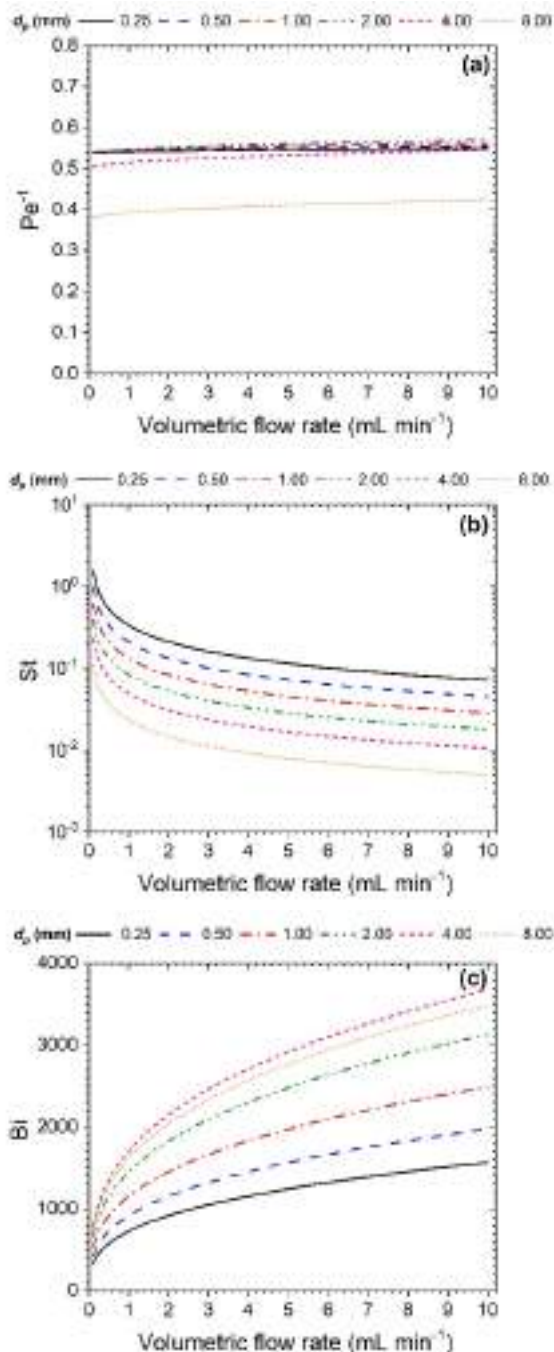


Figure 9. Effect of particle diameter on (a) Péclet number, (b) Stanton number, and (c) mass Biot number, using a PBR at 65 °C,  $[S] = 100$  g/L,  $[E] = 10$  g/L, and pH = 7.5.

## Conclusions

The mathematical model of the PBR was validated with experimental data. The model consisted in the inclusion of a particle model previously published and validated using immobilized and free enzyme in a STR, in which the Briggs-Haldane bioreaction is considered to occur within the porous network of the biocatalytic bead, where the kinetic and diffusive mechanisms were independently described.

During the bioconversion of glucose to fructose using immobilized enzyme, packed with CAB in a PBR, higher conversions are obtained at lower inlet flow rates, as the residence time of the glucose solution is longer. The conversion in a PBR can be improved, even higher than in a STR, prolonging the reaction time, with the advantage of increasing the reuse of the enzyme, compared to the STR.

Under the study conditions, in contrast to the effect exerted by diffusive mass transport on the specific productivity of fructose, the effect of the axial dispersion and the convective mass transport are negligible. Furthermore, as a result of the analysis of dimensionless numbers on the performance of the bioreactor, it was found that the Damköhler and Reynolds numbers exert the highest effect on the conversion of the bioprocess.

Increasing enzyme concentration promotes the fructose production; this effect is accentuated at low flow regimens in the PBR. However, specific productivity decreases, leading to a waste of the used enzyme.

Feed glucose concentration at a constant enzyme concentration showed the least effect on the bioconversion process compared to the other factors. This variable promotes a notable effect on productivity and the latter increases as feed concentration is raised. Higher lengths of the reactor drive higher glucose conversions; the highest conversions are obtained at low volumetric flow rates, despite greater amounts of enzyme are needed for higher lengths of the reactor. Specific productivity increases as packed bed lengths are shorter. Due to the high diffusional intraparticle resistance, the impact of a smaller catalytic bead size is highly relevant on the bioconversion, specially at low flow regimens.

The particle diameter was the only parameter that had a marked and positive effect on both conversion and productivity by reducing its size. The use of large particles represents a waste of catalyst, because the

center of those particles does not contribute to the overall glucose isomerization process. For selecting the smallest possible size in which beads hold their usefulness, the bead mechanical tolerance should be analyzed, taking care to avoid excessive pressure gradients, as well as to improve the immobilization technique to increase the effective diffusion within the particle.

## Acknowledgements

This research was supported by Programa de Fomento y Apoyo a Proyectos de Investigación (PROFAPI 2014/086 and PROFAPI 2015/118), Universidad Autónoma de Sinaloa.

## Nomenclature

$\hat{a}_p$	specific particle area (1/m)
Bi	mass Biot number
C	concentration (M)
$c_1$	substrate concentration (M)
$c_2$	product concentration (M)
CAB	calcium alginate beads
$c_{s,i}$	concentration at the particle surface (M)
$C_{feed,i}$	feed concentration (M)
$C_i$	liquid phase concentration (M)
$d_p$	diameter of the catalytic particle (m)
$d_t$	diameter of the bioreactor (m)
D	diameter (m)
Da	Damköhler number
$D_{AB}$	molecular diffusion coefficient (m <sup>2</sup> /s)
$D_{eff,i}$	effective diffusivity coefficient (m <sup>2</sup> /s)
$D_z$	axial dispersion coefficient (m <sup>2</sup> /s)
E	enzyme
[E]	enzyme concentration (g/L)
$[E]_{imm}$	immobilized (effective) enzyme concentration (g/L)
FREA	fraction of residual enzymatic activity
$j_m$	Colburn mass transfer coefficient
P	product
PBR	packed bed reactor
Pe	particle Péclet number
$Pe_z$	reactor Péclet number in z direction
Q	volumetric flow rate (mL/min)
r	radius (m)
$r_p$	radius of the bead (m)
$-r_1$	substrate consumption reaction rate (M/s)
$r_2$	product generation reaction rate (M/s)
$r_i$	reaction rate for free enzyme (M/s)

$\hat{f}_i$	reaction rate based on volume of bead pores (M/s)
$R^2$	coefficient of determination
Re	Reynolds number
$S$	substrate
$[S]$	substrate concentration (g/L)
Sc	Schmidt number
Sh	Sherwood number
St	Stanton number
STR	stirred tank reactor
$T$	temperature (°C)
$t$	time (s)
$k_1, k_{-2}$	intermediary reaction rate constants (1/(M·s))
$k_2, k_{-1}$	intermediary reaction rate constants (mol/(g·s))
$K_{eq}$	equilibrium constant
$k_{L,i}$	convective mass transfer coefficient (m/s)
$K_{mf}$	glucose to fructose Michaelis-Menten affinity constant (M)
$K_{mr}$	fructose to glucose Michaelis-Menten affinity constant (M)
$L$	reactor length (m)
$m_{E,t}$	total mass of immobilized enzyme (g)
$U_s$	surface velocity (m/s)
$V_{mf}$	glucose to fructose maximum reaction rate (M/s)
$V_{mr}$	fructose to glucose maximum reaction rate (M/s)
$V$	volume (L)
$V_p$	total beads volume (L)
$V_t$	total reaction volume (L)
$V_\infty$	supernatant volume (L)
$z$	axial direction

#### Greek letters

$\alpha$	significance level
$\varepsilon$	volumetric fraction of liquid phase (L/L)
$\varepsilon_p$	porosity of the bead (L/L)
$\varepsilon_b$	porosity of the packed bed (L/L)
$\mu$	viscosity of the fluid phase (kg/m·s)
$\eta$	fraction of residual enzymatic activity
$\rho$	density of the fluid phase (kg/m <sup>3</sup> )
$\rho_p$	density of the beads (kg/m <sup>3</sup> )
$\tau_{bed}$	residence time within the reactor (h)
$\tau_{diff}$	characteristic time for intraparticle diffusional mobility of the reactants (h)
$\tau_{mf}$	characteristic reaction time (h)

$\tau_{part}$	characteristic time for a fluid element to move from one particle extreme to the other in the axial direction (s)
$\tau_{st}$	time to reach the steady state (h)
$\Delta p$	pressure gradient (Pa)
<i>Subscripts</i>	
$i$	$i$ species (1 = glucose and 2 = fructose)
0	initial condition
$t$	total

## References

- Aguilar, R., Soto, G., Martínez, S. and Maya-Yescas, R. (2005). Substrate regulation in fixed bed bioreactors via feedback control. *Revista Mexicana de Ingeniería Química* 3, 1-11.
- Asif, M. (2015). Retrofitting of fixed-bed heterogeneous reactors for glucose isomerization. *Chemical Engineering Communications* 202, 1547-1556. <https://doi.org/10.1080/00986445.2014.959587>
- Asif, M. and Abasaed, A. E. (1998). Modeling of glucose isomerization in a fluidized bed immobilized enzyme bioreactor. *Bioresource Technology* 64, 229-235. [https://doi.org/10.1016/S0960-8524\(97\)00119-3](https://doi.org/10.1016/S0960-8524(97)00119-3)
- Bird, R. B., Stewart, W. E. and Lightfoot, E. N. (2006). *Transport Phenomena* rev 2nd Ed.
- Boudrant, J., Woodley J. M. and Fernandez-Lafuente R. (2020). Parameters necessary to define an immobilized enzyme preparation. *Process Biochemistry* 90, 66-80. <https://doi.org/10.1016/j.procbio.2019.11.026>
- Camacho-Rubio, F., Jurado-Alameda, E., González-Tello, P. and Luzón-González, G. (1995). Kinetic study of fructose-glucose isomerization in a recirculation reactor. *The Canadian Journal of Chemical Engineering* 73, 935-940. <https://doi.org/10.1002/cjce.5450730618>
- Cano-Sampedro, E., Pérez-Pérez, V., Osorio-Díaz, P., Camacho-Díaz, B. H., Tapia-Maruri D., Mora-Escobedo, R. and Alamilla-Beltrán, L. (2021). Germinated soybean protein hydrolysate: ionic gelation encapsulation and release under colonic conditions. *Revista Mexicana de Ingeniería*

- Química* 20, 725-737. <https://doi.org/10.24275/rmiq/Alim2319>
- Carrasco-Escalante, M., Caro-Corrales, J., Iribes-Salazar, R., Ríos-Irbe, E., Vázquez-López, Y., Gutiérrez-Dorado, R. and Hernández-Calderón, O. (2020). A new approach for describing and solving the reversible Briggs-Haldane mechanism using immobilized enzyme. *The Canadian Journal of Chemical Engineering* 98, 316-329. <https://doi.org/10.1002/cjce.23528>
- Che-Galicia, G., Martínez-Vera, C., Ruiz-Martínez, R. S. and Castillo-Araiza, C. O. (2014). Modelling of a fixed bed adsorber based on an isotherm model or an apparent kinetic model. *Revista Mexicana de Ingeniería Química* 13, 539-553.
- Chopda, V. R., Nagula, K. N., Bhand, D. V. and Pandit, A. B. (2014). Studying the effect of nature of glass surface on immobilization of glucose isomerase. *Biocatalysis and Agricultural Biotechnology* 3, 86-89. <https://doi.org/10.1016/j.bcab.2014.01.001>
- Chung, S. F. and Wen, C. Y. (1968). Longitudinal dispersion of liquid flowing through fixed and fluidized beds. *AIChE Journal* 14, 857-866. <https://doi.org/10.1002/aic.690140608>
- Dal Magro, L., Kornecki J. F., Klein M. P., Rodrigues R. C. and Fernandez-Lafuente R. (2020). Pectin lyase immobilization using the glutaraldehyde chemistry increases the enzyme operation range. *Enzyme and Microbial Technology* 132, 109397. <https://doi.org/10.1016/j.enzmictec.2019.109397>
- Dehkordi, A. M., Safari, I. and Karima, M. M. (2008). Experimental and modeling study of catalytic reaction of glucose isomerization: kinetics and packed-bed dynamic modeling. *AIChE Journal* 54, 1333-1343. <https://doi.org/10.1002/aic.11460>
- Dehkordi, A. M., Tehrany, M. S. and Safari, I. (2009). Kinetics of glucose isomerization to fructose by immobilized glucose isomerase (Sweetzyme IT). *Industrial & Engineering Chemistry Research* 48, 3271-3278. <https://doi.org/10.1021/ie800400b>
- Dormand, J. R., and Prince, P. J. (1980). A family of embedded Runge-Kutta formulae. *Journal of Computational and Applied Mathematics* 6(1), 19-26.
- Figuroa-García, E., Farias-Cervantes V., Segura-Castruita, M., Andrade-Gonzalez, I., Montero-Cortés, M. and Chávez-Rodríguez, A. (2021). Using artificial neural networks in prediction of the drying process of foods that are rich in sugars. *Revista Mexicana de Ingeniería Química* 20, 161-171. <https://doi.org/10.24275/rmiq/Sim1403>
- Gaily, M. H., Sulieman, A. K. and Abasaeed, A. E. (2013). Kinetics of a three-step isomerization of glucose to fructose using immobilized enzyme. *International Journal of Chemical Engineering and Applications* 4, 31. <https://doi.org/10.7763/IJCEA.2013.V4.255>
- Homaei, A. A., Sariri, R., Vianello, F. and Stevanato, R. (2013). Enzyme immobilization: an update. *Journal of Chemical Biology* 6, 185-205. <https://doi.org/10.1007/s12154-013-0102-9>
- Junqueira, L. L., De Brito, A. R., Franco, M. and De Assis, S. A. (2019). Partial characterization and immobilization of Carboxymethylcellulase from *Aspergillus niger* produced by solid-state fermentation. *Revista Mexicana de Ingeniería Química* 18, 241-250. <https://doi.org/10.24275/uam/izt/dcbi/revmexingquim/2019v18n1/Junqueira>
- Krishnamoorthi, S., Banerjee, A. and Roychoudhury, A. (2015). Immobilized enzyme technology: potentiality and prospects. *Journal of Enzymology and Metabolism* 1(1), 010-104.
- Nawaz, A., Sameer, M., Akram, F., Tahir, S., Arshad, Y., Haq, I. and Mukhtar, H. (2021). Kinetic and thermodynamic insight of a polygalacturonase: A biocatalyst for industrial fruit juice clarification. *Revista Mexicana de Ingeniería Química* 20, 1029-1045. <https://doi.org/10.24275/rmiq/Bio2355>
- Neifar, S., Cervantes, F. V., Bouanane-Darenfed, A., BenHlima, H., Ballesteros, A. O., Plou, F. J. and Bejar, S. (2020). Immobilization of the glucose isomerase from *Caldicoprobacter algeriensis* on sepabeads EC-HA and its

- efficient application in continuous high fructose syrup production using packed bed reactor. *Food Chemistry* 309, 125710. <https://doi.org/10.1016/j.foodchem.2019.125710>
- Palazzi, E. and Converti, A. (2001). Evaluation of diffusional resistances in the process of glucose isomerization to fructose by immobilized glucose isomerase. *Enzyme and Microbial Technology* 28(2-3), 246-252. [https://doi.org/10.1016/S0141-0229\(00\)00323-9](https://doi.org/10.1016/S0141-0229(00)00323-9)
- Peschke, T., Bitterwolf, P., Rabe, K. S. and Niemeyer, C. M. (2019). Self-immobilizing oxidoreductases for flow biocatalysis in miniaturized packed-bed reactors. *Chemical Engineering & Technology* 42, 2009-2017. <https://doi.org/10.1002/ceat.201900073>
- PonRani, V. M. and Rajendran, L. (2012). Mathematical modelling of steady-state concentration in immobilized glucose isomerase of packed-bed reactors. *Journal of Mathematical Chemistry* 50, 1333-1346. <https://doi.org/10.1007/s10910-011-9973-6>
- Rahman, N. Abd., Hussain, M. A. and Md.Jahim, J. (2013). Comparison study of experimental and simulation in the glucose isomerisation process in a fixed-bed reactor. *Advanced Materials Research* 781-784, 961-964. <https://doi.org/10.4028/www.scientific.net/amr.781-784.961>
- Ribeiro, A. M., Neto, P. and Pinho, C. (2010). Mean porosity and pressure drop measurements in packed beds of monosized spheres: side wall effects. *International Review of Chemical Engineering* 2, 40-46.
- Richit, L. A., Wolf, T. C., Ribeiro, M. C., Grzybowski, J. M., da Luz, C. and Dervanoski, A. (2020). Finite difference approximation in a non-isothermal and non-adiabatic fixed bed adsorption model: an application to n-hexane. *Brazilian Journal of Chemical Engineering* 37, 249-262. <https://doi.org/10.1007/s43153-020-00015-z>
- Santana, J. L., Oliveira, J. M., Nascimento, J. S., Mattedi, S., Krause, L. C., Freitas, L. S., Cavalcanti, E. B., Pereira, M. M., Lima, A. S. and Soares, C. M. F. (2020). Continuous flow reactor based with an immobilized biocatalyst for the continuous enzymatic transesterification of crude coconut oil. *Biotechnology and Applied Biochemistry* 67, 404-413. <https://doi.org/10.1002/bab.1885>
- Selvi, M. S. M. and Hariharan, G. (2016). Wavelet-based analytical algorithm for solving steady-state concentration in immobilized glucose isomerase of packed-bed reactor model. *The Journal of Membrane Biology* 249, 559-568. <https://doi.org/10.1007/s00232-016-9905-2>
- Singh, T. A., Jajoo, A. and Bhasin, S. (2020). Optimization of various encapsulation systems for efficient immobilization of actinobacterial glucose isomerase. *Biocatalysis and Agricultural Biotechnology* 29, 101766. <https://doi.org/10.1016/j.bcab.2020.101766>
- Tumturk, H., Demirel, G., Altinok, H., Aksoy, S. and Hasirci, N. (2008). Immobilization of glucose isomerase in surface-modified alginate gel beads. *Journal of Food Biochemistry* 32, 234-246. <https://doi.org/10.1111/j.1745-4514.2008.00171.x>
- Verduzco-Navarro, I., Jasso-Gastinel, C., Rios-Donato, N. and Mendizábal, E. (2020). Red dye 40 removal by fixed-bed columns packed with alginate-chitosan sulfate hydrogels. *Revista Mexicana de Ingeniería Química* 19, 1401-1411. <https://doi.org/10.24275/rmiq/IA1123>
- Wilson, E. J. and Geankoplis, C. J. (1966). Liquid mass transfer at very low Reynolds numbers in packed beds. *Industrial & Engineering Chemistry Fundamentals* 5, 9-14.
- Won, K., Kim, S., Kim, K. J., Park, H. W. and Moon, S. J. (2005). Optimization of lipase entrapment in ca-alginate gel beads. *Process Biochemistry* 40, 2149-2154. <https://doi.org/10.1016/j.procbio.2004.08.014>
- Yu, H., Guo, Y., Wu, D., Zhan, W. and Lu, G. (2011). Immobilization of glucose isomerase onto GAMM support for isomerization of glucose to fructose. *Journal of Molecular Catalysis B: Enzymatic* 72, 73-76. <https://doi.org/10.1016/j.molcatb.2011.05.006>

Zhang, Z., Zhang, S., Lee, W. J., Lai, O. M., Tan, C. P. and Wang, Y. (2020). Production of Structured triacylglycerol via enzymatic interesterification of medium-chain triacylglycerol and soybean oil using a pilot-scale solvent-free packed bed reactor. *Journal of the American Oil Chemists' Society*. <https://doi.org/10.1002/aocs.12319>

Zhao, H., Cui, Q., Shah, V., Xu, J. and Wang, T. (2016). Enhancement of glucose isomerase activity by immobilizing on silica/chitosan hybrid microspheres. *Journal of Molecular Catalysis B: Enzymatic* 126, 18-23. <https://doi.org/10.1016/j.molcatb.2016.01.013>